Magnetoresistance and Hall effect near the metal-insulator transition of n-type $Cd_{0.95}Mn_{0.05}Te$

Y. Shapira
Department of Physics and Astronomy, Tufts University, Medford, Massachusetts 02155
and Francis Bitter National Magnet Laboratory, Massachusetts Institute of Technology, Cambridge, Massachusetts 02139

N. F. Oliveira, Jr.
Instituto de Fisica, Universidade de São Paulo, Caixa Postal 20516, 01498 São Paulo, São Paulo, Brazil
and Francis Bitter National Magnet Laboratory, Massachusetts Institute of Technology, Cambridge, Massachusetts 02139

P. Becla
Francis Bitter National Magnet Laboratory, Massachusetts Institute of Technology, Cambridge, Massachusetts 02139

T. Q. Vu
Department of Physics and Astronomy, Tufts University, Medford, Massachusetts 02155
(Received 9 November 1989)

The magnetoresistance (MR) and Hall coefficient of n-type $Cd_{0.95}Mn_{0.05}Te$ samples with carrier concentrations $1.2\times10^{17}\le n\le6.6\times10^{17}$ cm^{-3} were measured at $1.2\le T\le4.2$ K in fields up to 200 kOe. The results at zero magnetic field show that the carrier concentration at the metal-insulator transition is $n_c\cong2\times10^{17}$ cm^{-3}, in rough agreement with Mott's prediction. In fields $H\lesssim80$ kOe the resistivity ρ first increases with H, then passes through a maximum, and finally decreases. The increase of ρ at low fields is accompanied by an increase in the magnitude of the Hall coefficient, while the decrease of ρ above the maximum is accompanied by an increase in the Hall mobility. The MR below ~80 kOe is attributed to mechanisms associated with the giant spin splitting of the conduction band. The increase of ρ at low fields follows the behavior expected from quantum corrections to the conductivity arising from the electron-electron interaction. The decrease of ρ above the maximum is attributed to the rise of the Fermi energy in the majority-spin subband. Above ~80 kOe the qualitative behavior of the MR depends on the carrier concentration. Samples with $n<n_c$ exhibit an upturn in the resistivity at high fields. This effect is attributed to the squeezing of the donor-electron wave function. In addition, the MR of these samples shows an anomaly near the first magnetization step. In metallic samples ($n>n_c$) the MR and Hall coefficient exhibit oscillations at high fields. The oscillations are interpreted as Shubnikov–de Haas oscillations arising from the majority-spin subband. This interpretation is supported by model calculations.

I. INTRODUCTION

The distinctive properties of magnetic semiconductors (MS's) and dilute magnetic semiconductors (DMS's) arise from the s-d interaction. This interaction couples the spins of s-like conduction electrons (or p-like holes) to the spins of $3d$ (or $4f$) localized magnetic ions. The striking magneto-optical and magnetotransport effects which are caused by this interaction were investigated since the 1960s, first in MS's,[1,2] and more recently in DMS's.[3–5] Investigations of DMS's have focused primarily on II-VI compounds in which some of the cations were replaced by Mn, and more recently by Fe or Co. DMS's enjoy some advantages over MS's, including a well-known band structure and a substantial body of knowledge concerning the parent compounds. In addition, the low-temperature mobility in some of the DMS's is much higher. These advantages are partially responsible for the rapid progress in the area of DMS's during the last decade.

In this paper we report the observation of several magnetoresistance (MR) phenomena in n-type $Cd_{1-x}Mn_xTe$ samples with carrier concentrations near the metal-insulator (M-I) transition. These data were obtained at temperatures $1.2\le T\le4.2$ K, in magnetic fields H up to ~200 kOe. Hall data are also reported. The effects observed at relatively low magnetic fields ($H\lesssim80$ kOe) are attributed to several mechanisms associated with the giant spin splitting of the conduction band. The various phenomena which are observed at higher fields are attributed to the squeezing of the donor-electron wave function by the magnetic field, to magnetization steps, and to Landau quantization of the electrons in the majority-spin subband.

Previous studies of the MR in n-type wide-band-gap DMS's were mainly devoted to $Cd_{1-x}Mn_xSe$.[6–13] The present work on n-type $Cd_{1-x}Mn_xTe$ confirmed many of these earlier results, but it also uncovered new MR effects at higher magnetic fields. To put the present work in context, we summarize some of the relevant findings in n-type $Cd_{1-x}Mn_xSe$ and in other DMS's.

Much of the work on n-type $Cd_{1-x}Mn_xSe$ was on samples with carrier concentrations not far from the M-I

transition. These studies were carried out in magnetic fields $H < 80$ kOe. The salient features observed at temperatures $0.3 \leq T \leq 4$ K were a positive MR at low fields, followed by a decrease of the resistivity ρ at higher fields. This behavior has been attributed to several mechanisms associated with the giant spin splitting of the conduction band in a magnetic field.[8,9,11–13] The specific mechanisms which seem to dominate will be discussed later in connection with the interpretation of similar data for the present $Cd_{1-x}Mn_xTe$ samples.

An additional MR effect was previously observed in $Cd_{1-x}Mn_xSe$ samples which were on the insulating side of the *M-I* transition.[6] At low temperatures the resistivity of these samples showed an upturn at high magnetic fields. This upturn has been attributed to the squeezing of the donor wave function by the magnetic field—a well-known effect which is present also in nonmagnetic semiconductors.[14] The effect was also observed in *n*-type CdSe, i.e., in the absence of manganese.[6] In this paper we report similar observations in *n*-type $Cd_{1-x}Mn_xTe$ samples which are on the insulating side of the *M-I* transition.

Shubnikov–de Haas (SdH) oscillations have been studied in narrow-band-gap DMS's, $Hg_{1-x}Mn_xTe$ and $Hg_{1-x}Mn_xSe$, which have high mobilities.[15] However, to our knowledge such oscillations have not been observed previously in wide-band-gap DMS's, which have lower mobilities. Here we report the observation of SdH oscillations (albeit only two cycles) in samples which are on the metallic side of the *M-I* transition. The period of the oscillations is consistent with that expected from the majority subband.

Recent work has shown that at low temperatures the magnetization curve, *M versus H*, of a DMS exhibits steps at high magnetic fields.[16] A magnetoresistance anomaly near a magnetization step was observed in $Hg_{1-x-y}Cd_xMn_yTe$.[17] Here we report the observation of a MR anomaly near the first magnetization step. The anomaly was found in samples which were on the insulating side of the *M-I* transition.

This paper is organized as follows. The experimental techniques are described in Sec. II. The room-temperature properties of the samples, and zero-field resistivity data at $1.2 \leq T \leq 4.2$ K, are reported in Sec. III. The MR and Hall data, and their interpretation, are presented in two sections: Sec. IV focuses on the effects at $H \lesssim 80$ kOe, whereas Sec. V is devoted to the effects at higher fields.

II. EXPERIMENTAL TECHNIQUES

Experiments were carried out on *n*-type single crystals of $Cd_{1-x}Mn_xTe$, grown by the Bridgman method. These crystals were intentionally doped with both In and Al, except for one crystal (no. 4) which was doped with In only. The [In/Al] ratio was about 10. The reason for using both In and Al was that somewhat higher carrier concentrations could be achieved, as compared to doping with In only. The nominal Mn concentration for all the samples was $x = 0.05$. The actual values of x, determined by atomic absorption, varied between $x = 0.044$ and 0.050.

Thin slices (about 1 mm in thickness) were cut from the boules. These slices were annealed at 600 °C under Cd pressure for periods between 1 and 10 d. Bar-shaped samples for the resistivity and Hall measurements were cut from the annealed slices. The resistivity and Hall measurements were made using standard dc techniques, described in Ref. 11. Data from 1.2 to 4.2 K were taken with the samples immersed in liquid ^{4}He.

Two different magnets were used: a high-field Bitter magnet, and a Nb-Ti superconducting magnet. Much of the data were acquired continuously during field sweeps in both magnets, but the most accurate data at low fields were taken point by point using the superconducting magnet. All data were taken with the magnetic field **H** perpendicular to the current through the sample.

III. BEHAVIOR AT ZERO MAGNETIC FIELD

The electrical properties of the samples at room temperature (RT) are given in Table I. They include the carrier concentration n_{RT}, the resistivity ρ_{RT}, and the mobility μ_{RT}. The values for n_{RT} are from Hall measurements. The values of ρ_{RT} and μ_{RT} are subject to an uncertainty of 15%, typically. This uncertainty is related to the finite size of the voltage contacts, which leads to an uncertainty in their separation. Also given in Table I are the Mn concentration x (from atomic absorption), the zero-field resistivity at 4.2 K, and the dopants (In and Al, or In only). The samples listed as 5A and 5B were both cut from the same annealed slice.

The temperature variation of the zero-field resistivity for $1.2 \leq T \leq 4.2$ K is shown in Fig. 1. These data suggest that the carrier concentration at the *M-I* transition is $n_c \cong 2 \times 10^{17}$ cm^{-3} for $x \cong 0.05$. This result should be

TABLE I. Electrical properties of the $Cd_{1-x}Mn_xTe$ samples at $H = 0$. Room-temperature carrier concentration n_{RT}, resistivity ρ_{RT}, and Hall mobility μ_{RT}. The Mn concentration x is from atomic absorption. $\rho_{4.2\,K}$ is the resistivity at 4.2 K.

Sample no.	x	Dopants	n_{RT} (cm^{-3})	ρ_{RT} (Ω cm)	μ_{RT} (cm^2/V s)	$\rho_{4.2\,K}$ (Ω cm)
1	0.050	In,Al	1.2×10^{17}	0.20	260	40
2	0.045	In,Al	1.7×10^{17}	0.135	270	3.3
3	0.050	In,Al	2.1×10^{17}	0.124	240	0.8
4	0.048	In	2.9×10^{17}	0.033	650	0.06
5A	0.044	In,Al	5.9×10^{17}	0.023	460	0.035
5B	0.044	In,Al	6.6×10^{17}	0.020	470	0.026

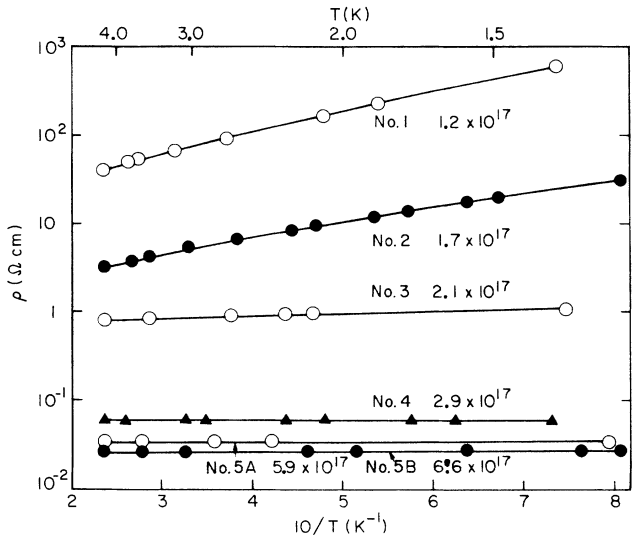

FIG. 1. Temperature variation of the resistivity ρ at zero magnetic field. The room-temperature carrier concentration n_{RT} (in electrons/cm^3) is indicated next to the sample number.

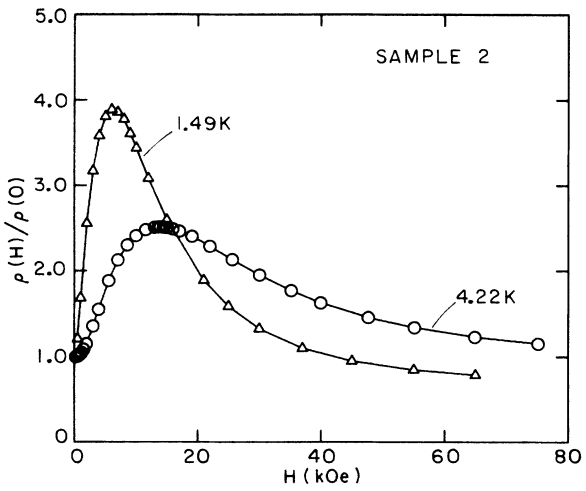

FIG. 2. Magnetoresistance of sample 2 at 4.22 and 1.49 K.

compared with the expected value $n_c \cong 1\times10^{17}$ cm^{-3} for CdTe, obtained from Mott's relation[18]

$$n_c \cong (0.26/a_H)^3 , \quad (1)$$

where a_H is the effective Bohr radius for the donor. To obtain a_H we used $m^*=0.10m_0$ for the electron effective mass, and a low-temperature static dielectric constant $\kappa=10$.[19,20] The factor-of-2-higher n_c estimated from the data in Fig. 1 is consistent with the previously observed increase of n_c with increasing x.[11,12] The Mott minimum metallic conductivity[18] for CdTe is $\sigma_c=5$ $(\Omega\,\text{cm})^{-1}$, corresponding to $\rho_c=0.2$ Ω cm. The data in Fig. 1, which are at relatively high temperatures, are consistent with this value.

IV. MAGNETORESISTANCE AND HALL EFFECT BELOW ~80 kOe

A. Experimental results

Examples of the MR below ~80 kOe are shown in Fig. 2. As H increases, the resistivity ρ first increases, then goes through a maximum, and finally decreases. These qualitative features were observed in all the samples at temperatures from about 1.2 to 4.2 K.

Examination of the MR data for all the samples shows the following general trends. (1) The field H_{max}, where the resistivity is at its maximum, decreases as T decreases. (2) At a fixed T, the field H_{max} increases slowly with increasing carrier concentration. The only exception is sample 4. This exception may be related to the fact that sample 4, unlike the others, was doped with In only. (3) The ratio $\rho(H_{max})/\rho(H=0)$ increases with decreasing T, in this temperature range. (4) The magnitude of the MR is much smaller for samples with $n \gg n_c$ (samples 5A and 5B) than in samples with $n \lesssim n_c$. These general trends are similar to those observed earlier in $Cd_{1-x}Mn_xSe$ under similar conditions.[11,12]

Figure 3 shows the Hall coefficient R and the Hall mobility $\mu=|R/\rho|$ which correspond to the MR at 4.22 K in Fig. 2. These data indicate that the positive MR in fields below H_{max} is associated with a large increase of $|R|$. On the other hand, the decrease of ρ in fields above H_{max} is largely due to an increase of μ.

B. Theoretical models for the MR below ~80 kOe

The qualitative features of the MR of the present samples, in fields $H \lesssim 80$ kOe, are similar to those observed earlier in n-type $Cd_{1-x}Mn_xSe$.[6–13] The main causes of

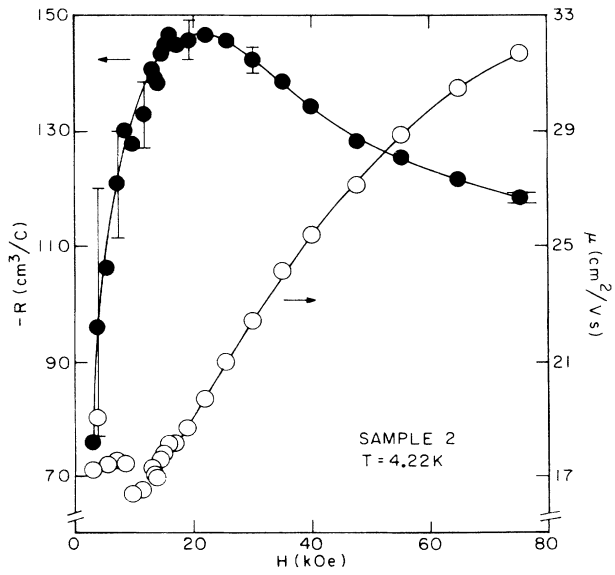

FIG. 3. Magnetic field dependence of the Hall coefficient R (solid circles) and the Hall mobility μ (open circles) for sample 2 at 4.22 K.

this MR are believed to be related to the giant spin splitting of the conduction band (CB), which occurs when a magnetic field is applied.[7–9,11–13] The present theoretical understanding of the MR is based mostly (but not entirely) on models for metallic samples, with carrier concentrations n close to but higher than n_c. The MR of samples with n slightly below n_c (which is qualitatively similar to the MR of metallic samples) is presumed to arise from similar mechanisms.

1. Spin splitting of the conduction band

The spin splitting of the CB is sketched in Fig. 4. The splitting is almost entirely due to the s-d interaction. This interaction leads to a splitting energy δ which is proportional to the magnetization M (see, e.g., Refs. 3–5). In the field range under consideration, δ is well represented by the equation

$$\delta=\delta_x(M/M_s)\ , \tag{2}$$

where δ_x varies from about 11 meV for $x=0.03$ to about 16 meV for $x=0.05$.[21,22] The ratio M/M_s in Eq. (2), which is the magnetization divided by the technical saturation value,[16] is well approximated by[21]

$$M/M_s=B_{5/2}[5\mu_B H/k_B(T+T_0)]\ , \tag{3}$$

where $B_{5/2}$ is the Brillouin function for spin $\frac{5}{2}$, μ_B is the Bohr magneton, k_B is the Boltzmann constant, and T_0 is a phenomenological parameter. For $Cd_{1-x}Mn_xTe$ the value of T_0 when x is near 0.05 is approximately $T_0=47x$, where T_0 is in units of K.[21,22] For a given x, the technical saturation value M_s is a constant.

In theoretical models for metallic samples the relative magnitudes of the spin splitting δ, the thermal energy k_BT, and the Fermi energy E_F, are important. In the present experiments, $k_BT<0.4$ meV, which is much smaller than $E_F\sim 20$ meV for the metallic samples. The magnetic field necessary to produce a splitting δ comparable to k_BT is about 1 kOe at 4.2 K, and is still lower at lower temperatures. Substantially higher fields are necessary to produce a splitting δ comparable to E_F. For fields near 80 kOe and when $T\leq 4.2$ K, the Brillouin function in Eq. (3) is nearly saturated so that $\delta\cong\delta_x\cong 15$ meV. Such a splitting is comparable to the Fermi energy $E_F(0)$ at $H=0$. [For a parabolic band with $m^*=0.10m_0$, $E_F(0)$ varies between 16 and 26 meV when n varies between 3×10^{17} and 6×10^{17} cm^{-3}.] For fields near H_{max}, $\delta\gtrsim 5$ meV in the present experiments.

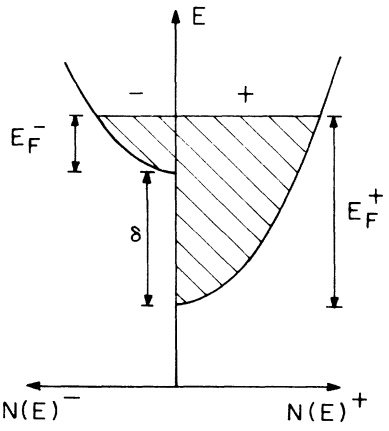

FIG. 4. Schematic showing the spin splitting of the conduction band. E is the energy. $N^+(E)$ and $N^-(E)$ are the densities of states for the majority (+) and minority (−) spin subbands, respectively. δ is the spin-splitting energy. E_F^+ and E_F^- are the Fermi energies of the subbands. The shaded area represents occupied states.

2. MR mechanisms associated with the spin splitting of the CB

The MR mechanisms associated with the spin splitting of the CB in wide-gap DMS's can be divided into two groups. First, there is a positive MR associated with the quantum corrections to the conductivity which arise from the electron-electron interaction. This mechanism was proposed by Sawicki *et al.* and Dietl *et al.*[8,9,13] The data presented by these authors, on n-type $Cd_{1-x}Mn_xSe$, suggest that it is the dominant MR mechanism at low fields where δ is of the order k_BT. Even at higher fields this mechanism is important, although it cannot be the cause of the decrease of the resistivity in fields above H_{max}. The rise of the Hall coefficient at low fields can also be explained, at least qualitatively, with this mechanism.[8]

Second, there are MR mechanisms associated with the redistribution of electrons between the two spin subbands.[12] As shown in Fig. 4, the splitting δ causes electrons to shift from the minority-spin subband (−) to the majority-spin subband (+). This redistribution of electrons is substantial when δ is a sizeable fraction of $E_F(0)$. Thus, the effects of the electron redistribution are believed to be particularly important in fields $H>H_{max}$.

The redistribution of electrons, between the spin subbands, can affect the resistivity in several ways. One mechanism, discussed by Fukuyama and Yosida,[23] focuses on the fact that the mobility of an electron increases with energy. This is especially true for samples with $n<n_c$, in which the mobility depends strongly on the energy separation from the mobility edge. As δ increases, the electron redistribution raises the Fermi energy E_F^+ in the majority-spin (+) subband, and lowers E_F^- in the minority-spin (−) subband. (For either subband, E_F is measured from the bottom of that subband.) The rise of E_F^+ increases the mobility in the majority-spin subband, and the fall of E_F^- lowers the mobility in the minority-spin subband. It was shown by Fukuyama and Yosida that when the contributions of both subbands are added, the net effect of the changes in the Fermi energies is a negative MR, i.e., the rise of E_F^+ dominates. This is the most likely cause of the decrease of the resistivity in fields above H_{max}, particularly for the samples with $n<n_c$ in which the Fukuyama-Yosida mechanism is expected to be important.

Other treatments of the MR associated with the electron redistribution focus on the resistivity due to ionized impurity scattering. An early model by Shapira and Kautz[24] used the Brooks-Herring formula for ionized impurity scattering, and the Thomas-Fermi approximation for the screening radius. In this model there are two competing MR effects: the change in the screening radius with δ tends to produce a positive MR, while the changes of $E_F^{\pm}$ tend to produce a negative MR. Estimates based on a simple parabolic conduction band show that for the present metallic samples the MR should be negative and of the order 10%. This is comparable to the observed decrease of the resistivity above $H_{\max}$ in these metallic samples. For the samples with $n < n_c$, the observed decrease of ρ above $H_{\max}$ is much larger (see Fig. 2). For these samples, a stronger dependence of the mobility on energy must be assumed, as in the Fukuyama-Yosida model.

Larger MR effects can arise when exchange effects, neglected by Shapira and Kautz, are included in the treatment of ionized impurity scattering. When the conduction band splits, the screening of ionized donors is mostly by "+" electrons. Exchange effects then cause the scattering of + electrons to be stronger than that of "−" electrons. This effect was discussed by Kim and Schwartz in the context of ferromagnetic metals,[25] and by Gan and Lee[26] in the context of DMS's. The sign of the MR at low fields depends on the choice of parameters. For large δ, when the conduction is predominantly due to the majority (+) subband, we expect that exchange effects will lead to a positive MR.

There is no clear evidence that exchange effects are important in the present experiments. First, as discussed later, the MR at very low H ($\delta \lesssim k_B T$) follows the behavior expected from the quantum corrections to the conductivity. This implies that the MR effects associated with the redistribution of electrons between the two spin subbands (including the exchange effects) are not important in this low-field region. Even at high fields, but below $H_{\max}$, the quantum corrections mechanism seems to dominate. Finally, at fields above $H_{\max}$ the resistivity decreases with H. Such a negative MR is not expected from exchange effects in the region of large δ, but is expected from the mechanism involving the rise of E_F^+.

3. *Tests of predictions based on quantum corrections to the conductivity*

As mentioned, Sawicki *et al.* and Dietl *et al.*[8,9,13] attribute the positive MR in fields $H < H_{\max}$ to the effect of the CB spin splitting on the quantum corrrections to the conductivity. The relevant correction in this case is that due to the electron-electron interaction (not the correction due to interference). The theory of the positive MR associated with the interaction term was developed earlier.[27–29] The dominant contribution in the present case is expected to be due to particle-hole diffusion. Other contributions are expected to be smaller and they should not change the T and H dependences of the MR significantly, although they will have a small effect on the magnitude of the MR. For this reason we focus solely on the MR due to the particle-hole channel. This MR was first discussed by Lee and Ramakrishnan (LR).[27,28] Their theory indicates that the spin splitting of the CB leads to a change in the conductivity, $\Delta\sigma(H)$, which is given by

$$\Delta\sigma(H) = -AT^{1/2} g_3(h) , \tag{4}$$

where A is a positive constant which does not depend on T or H, and $g_3(h)$ is a definite integral involving $h = \delta(H)/k_B T$. Analytical expressions for $g_3(h)$ can be given in two limits:

$$g_3(h) = 0.0564 h^2, \quad \text{when } h \ll 1 \tag{5}$$

and

$$g_3(h) = h^{1/2} - 1.3, \quad \text{when } h \gg 1 . \tag{6}$$

The prefactor 0.0564 in Eq. (5), from our calculations, differs slightly from 0.053 given by LR.

The value of $g_3(h)$ for an aribitrary h can be obtained by numerical integration. Our numerical results show that Eq. (5) is actually a good approximation over a much wider range than is implied by the condition $h \ll 1$. The deviations at $h = 1$, 2, and 2.5 are 2.5, 9, and 14%, respectively [the actual values are smaller than those given by Eq. (5)]. When Eq. (5) applies, one can use Eqs. (2) and (4) to obtain

$$\Delta\sigma(H) = -a (M/M_s)^2 / T^{3/2} , \tag{7}$$

where

$$a = 0.0564 A \delta_x^2 / k_B^2 . \tag{8}$$

The value of M_s in Eq. (7) depends only on x, and is independent of T or H. Equation (7) therefore implies that, at low H, $\Delta\sigma$ is proportional to $M^2/T^{3/2}$. For large H, where $\delta/k_B T \gg 1$, Eqs. (4) and (6) give

$$\Delta\sigma(H) \propto -[\delta^{1/2} - 1.3(k_B T)^{1/2}] , \tag{9}$$

which means that $\Delta\sigma(H)$ is linear in $M^{1/2}$ at high fields.

The preceding theoretical predictions are for samples which are well in the metallic region, i.e., $k_F l_e \gg 1$, where k_F is the Fermi momentum and l_e is the elastic mean free path. Experimental tests of these predictions, however, were usually carried out on samples which were metallic but not too far from the *M-I* transition, i.e., $k_F l_e \sim 1$. The reason is that samples with $k_F l_e \gg 1$ have a very small MR. The prediction that $\Delta\sigma$ is linear in $\delta^{1/2}$, for large δ, was verified in several nonmagnetic semiconductors.[30,31] Both this prediction and the prediction for low δ were verified by Sawicki *et al.* in *n*-type $Cd_{1-x}Mn_xSe$.[8]

A test of Eq. (7) was carried out on sample 4. Between 4.2 and 1.3 K the resistivity of this sample increases only by 1%, showing that the sample is metallic. However, the sample is not too far from the *M-I* transition: the ratio between the conductivity at 4.2 K and Mott's minimum metallic conductivity is only 3, and $k_F l_e = 1$. The MR of this sample was measured at four temperatures between 4.2 and 1.6 K in low magnetic fields. The results for $\Delta\sigma(H)/\sigma(0)$ as a function of H^2 are shown in Fig. 5(a). These data show that $\Delta\sigma/\sigma$ is proportional to

H^2 at low H, with a proportionality constant which increases rapidly with decreasing T. The highest values of δ/k_BT for the four data sets in Fig. 5(a) are about 2.5 (i.e., $h \lesssim 2.5$), so that a comparison of these data with Eq. (7) is reasonable.

Figure 5(b) shows the same data plotted as a function of $(M/M_s)^2/T^{3/2}$. Here, M/M_s was calculated from Eq. (3) using the value $T_0=2.26$ K for this Mn concentration. The results in Fig. 5(b) show that the data for all four temperatures lie close to a single straight line which passes through the origin. This is precisely the behavior which is expected from Eq. (7) at low fields.

The confirmation of Eq. (7) is a very strong evidence that the positive MR at low fields arises mainly from the quantum corrections to conductivity, due to the interaction term. Although other mechanisms can also give rise to a MR which is proportional to M^2 at low M (because the MR is even in M), the $1/T^{3/2}$ factor in Eq. (7) is specific to these quantum corrections.

The magnitude of the MR in Fig. 5(b) is also in agreement with theoretical estimates. The prefactor A in Eq. (4) can be evaluated using equations given in Refs. 27–29 and the known properties of the sample [n, $\sigma(0)$, and m^*]. The only unknown factor is the interaction strength parameter $\tilde{F}_\sigma$ (cf. Ref. 28), which is expected to be of order 1. The magnitude of the MR calculated by setting $\tilde{F}_\sigma=1$ is only a factor of 2 smaller than that observed.

A test of the LR predictions for fields higher than those in Fig. 5 was also carried out on sample 4. In this test the MR was measured at 4.22 K in fields up to 76 kOe generated by the superconducting magnet. The results for $\Delta\sigma(H)/\sigma(0)$ *versus* $(M/M_s)^{1/2}$ are shown in Fig. 6. [The choice of $(M/M_s)^{1/2}$ as the variable is motivated by Eq. (9).] The value of δ_x for sample 4 is 15.3 meV, so that Fig. 6 corresponds to values of $h=\delta/k_BT$ up to about 40. The condition $\delta=k_BT$ is met at $(M/M_s)^{1/2}=0.15$.

The minimum of σ in Fig. 6 corresponds to the maximum resistivity at $H_{\max}$. As discussed earlier, the increase of σ (negative MR) at higher fields is attributed to the rise of E_F^+, which is an entirely different mechanism than the quantum corrections considered by LR. Thus, the comparison with the LR theory is only meaningful for fields well below the minimum of σ.

To find out the range over which the quantum corrections discussed by LR dominate the MR, the following procedure was used. The parameter a in Eq. (7) was obtained from the data in Fig. 5. The value of the parameter A in Eq. (4) was then calculated from Eq. (8) and the known value of δ_x. The LR prediction for $\Delta\sigma$ as a function of $(M/M_s)^{1/2}$ was then obtained from Eq. (4) using Eq. (2) to relate M/M_s to h, and the numerical results for $g_3(h)$. In essence this procedure is an extrapolation of the data in Fig. 5 to higher fields using the numerical results for $g_3(h)$. There are no adjustable parameters in this extrapolation.

The results of the extrapolation are given by the dashed line in Fig. 6. It represents the expected change

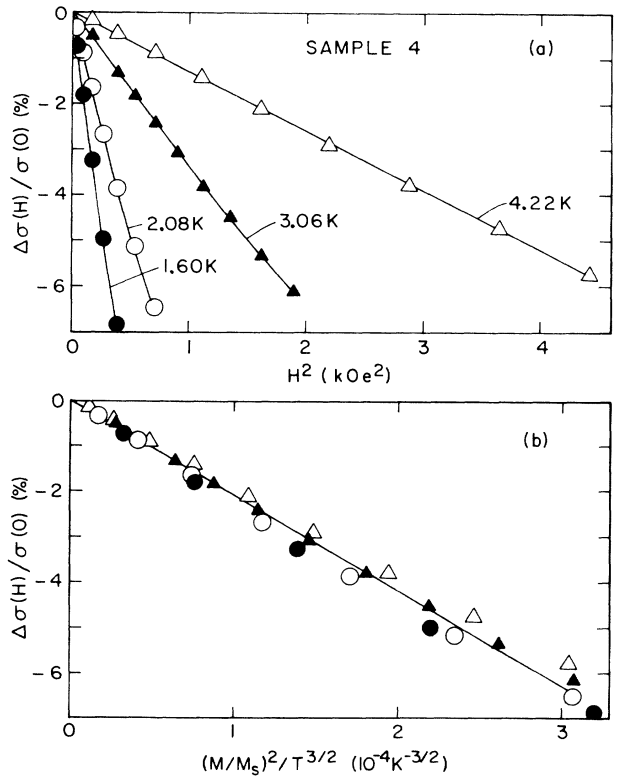

FIG. 5. (a) Fractional change in the conductivity, $\Delta\sigma(H)/\sigma(0)$, as a function of H^2 for sample 4 at four temperatures. (b) The same data plotted as a function of $(M/M_s)^2/T^{3/2}$, where M is the magnetization, M_s is the technical saturation value of M, and T is the temperature.

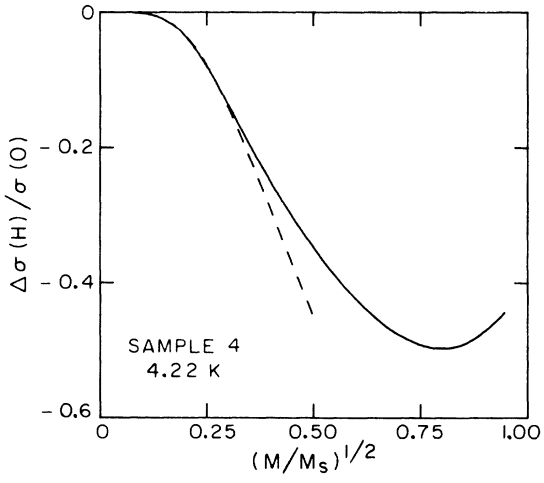

FIG. 6. Fractional change in the conductivity, $\Delta\sigma(H)/\sigma(0)$, as a function of $(M/M_s)^{1/2}$ for sample 4 at 4.22 K. These data correspond to fields up to 76 kOe. The dashed curve represents the expected variation due to quantum corrections, calculated by extrapolating the data in Fig. 5 using the Lee-Ramakrishnan theory (see text).

in σ due to the quantum corrections discussed by LR. A comparison with the experimental data indicates that this mechanism dominates the MR over a substantial range of $(M/M_s)^{1/2}$, at least up to 0.5 where $\delta/k_BT \cong 10$. The sign of the deviation at higher fields indicates that the competing mechanism gives rise to a MR of opposite sign (negative MR). Thus, there is no evidence for another important positive MR mechanism, i.e., the quantum corrections discussed by LR seem to be the dominant cause of the positive MR at all fields below H_{max}.

4. *Summary and conclusions*

The preceding analysis leads to the following conclusions. The positive MR at low fields ($\delta \lesssim k_BT$) is due to the effect of the spin splitting of the CB on the quantum corrections arising from the interaction term. Even at higher fields, but below H_{max}, this seems to be the dominant mechanism for the positive MR. These conclusions agree with those reached earlier by Dietl *et al.* and Sawicki *et al.* in their study of *n*-type $Cd_{0.95}Mn_{0.05}Se$. The negative MR above H_{max} is probably due to the rise of E_F^+ which accompanies the electron redistributions between the spin subbands. The change in the Thomas-Fermi screening radius, and exchange effects in ionized impurity scattering, do not seem to dominate the MR at any field below ~80 kOe.

V. MAGNETORESISTANCE AT HIGH FIELDS

The qualitative behavior of the MR for $H \gtrsim 80$ kOe depends on the carrier concentration. Three effects are observed in this field range. (1) For samples with $n < n_c$ the resistivity exhibits an upturn at the highest fields. (2) In these samples, as well as in sample 3 (with $n \cong n_c$), an anomaly in the resistivity is observed near the first magnetization step. (3) In metallic samples ($n > n_c$) the resistivity shows oscillations at high fields. Each of these three effects will be dicussed separately.

A. Upturn of the resistivity in high fields

In some samples the resistivity exhibits an upturn in high fields. This effect was observed in sample 1 at 4.2 and 1.3 K, and in sample 2 at 4.2 K. Both of these samples have carrier concentrations below n_c, i.e., they exhibit hopping conduction at low temperatures (see Fig. 1). An example of the upturn of the resistivity is shown in Fig. 7. The upturn is attributed to the squeezing of the donor-electron wave function by the high magnetic field.[6] This mechanism is not related to the *s-d* interaction, and is not specific to DMS's.[14]

B. MR anomaly near the first magnetization step

At low temperatures the magnetization curve, *M versus H*, of a DMS exhibits steps at high magnetic fields. The steps arise from energy-level crossings for pairs of nearest-neighbor Mn^{2+} ions.[16] In $Cd_{1-x}Mn_xTe$, with $x = 0.05$, the first step is near 104 kOe, and the second is near 195 kOe. Because the width of each step increases with temperature, these steps are resolved only at $T \lesssim 2$ K.

A weak MR anomaly was observed at the first magnetization step in samples 1 and 2 (both with $n < n_c$). The anomaly was also observed, but less clearly, in sample 3 ($n \cong n_c$). Figure 8 shows the results in sample 2. The anomaly appears as a slight increase of the negative slope of the MR curve. This is more readily seen in Fig. 9 which shows the derivative $-\partial\rho/\partial H$ of the data in Fig. 8. The observations of the anomaly associated with the

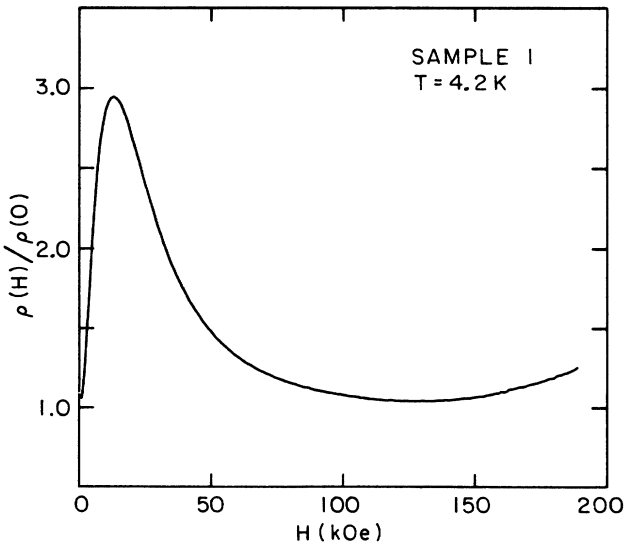

FIG. 7. Magnetoresistance of sample 1 at 4.2 K, showing the upturn of the resistivity at high fields.

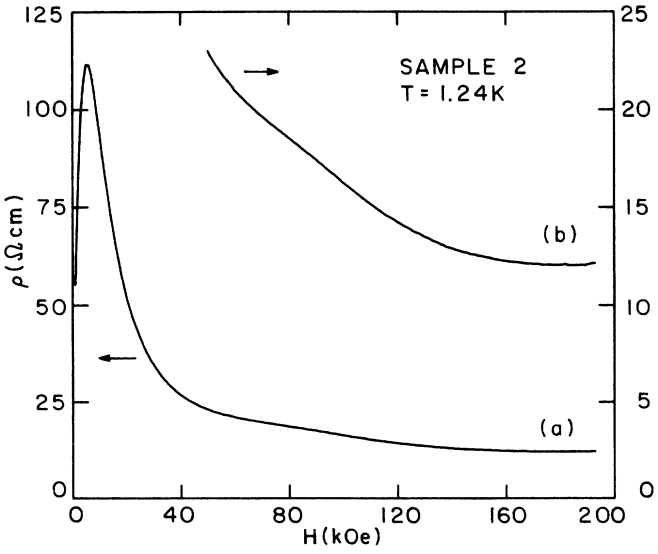

FIG. 8. (a) Magnetoresistance of sample 2 at 1.24 K. (b) Expanded view of the data near the first magnetization step at 104 kOe.

first magnetization step were made at $1.2 < T < 1.4$ K. As expected, no such anomaly was found at 4.2 K.

The results in Figs. 8 and 9 are interpreted as follows. In the field region where the anomaly is observed, the MR due to the *s-d* interaction is negative. The mechanism causing this negative MR is probably the rise of E_F^+ with increasing M. Because a magnetization step is associated with an increase in the slope dM/dH, it leads to an increase in the magnitude of $d\rho/dH = (d\rho/dM)(dM/dH)$.

No magnetoresistance anomaly was observed near the second magnetization step at 195 kOe. There are two reasons for this. First, the magnetization step at 195 kOe is near the very top of the available field range. Thus, at best no more than a portion of the anomaly associated with this step could have been observed. Second, the MR anomaly associated with the second step was probably masked by the positive MR associated with the squeezing of the donor wave function. This positive MR is not related to the magnetization, so that it should not be affected by the magnetization step. The strong H dependence of the positive MR tends to mask the weak anomaly in the negative MR near the second step. For sample 1 the upturn of the resistivity ρ as a function of H starts well before the second magnetization step, i.e., the positive MR dominates the behavior near the second step. For sample 2 (Fig. 8), the positive and negative MR mechanisms seem to balance each other near the second magnetization step.

C. Shubnikov–de Haas oscillations in metallic samples

The MR of the three metallic samples (nos. 4, 5A, and 5B) exhibited oscillations at high magnetic fields. The oscillations were observed both at 4.2 and 1.3 K, but were slightly more pronounced at the lower temperature. The oscillations consisted of only two cycles, even at the lowest temperature. Figure 10 shows the result for sample 4. Corresponding oscillations, but with a different phase angle, were also observed in the magnitude of the Hall coefficient. An example of the oscillations in the Hall coefficient is shown in Fig. 11.

The observed oscillations are interpreted as SdH oscillations. They arise from Landau levels in the majority-spin subband, although some contribution from the minority-spin subband cannot be ruled out. This interpretation is based on the model calculations described below. SdH oscillations are known to be periodic, or very nearly periodic, in $1/H$ (Ref. 32). The observed period, estimated with an accuracy of several percent, was

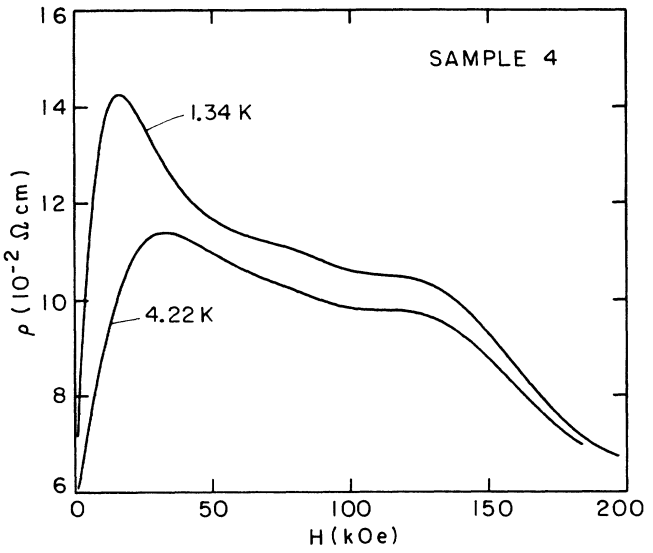

FIG. 10. Magnetoresistance of sample 4 at 4.22 and 1.34 K, showing the oscillatory behavior at high fields.

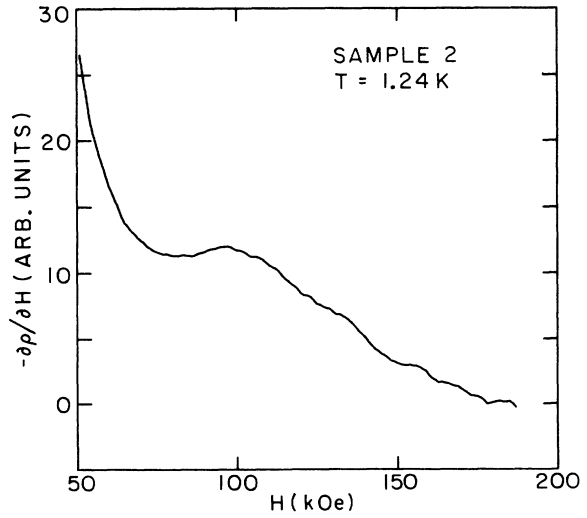

FIG. 9. The derivative $-\partial\rho/\partial H$ obtained by numerical differentiation of the data in Fig. 8.

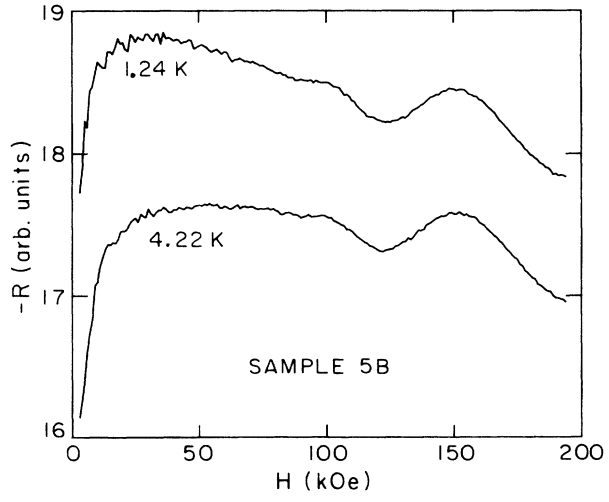

FIG. 11. Magnetic field dependence of the Hall coefficient R of sample 5B at 4.22 and 1.24 K, showing the oscillatory behavior at high fields.

$\Delta H^{-1}=4.8\times10^{-6}$ Oe^{-1} for sample 4, 3.6×10^{-6} Oe^{-1} for sample 5A, and 3.3×10^{-6} Oe^{-1} for sample 5B. The model calculations show that these periods are close to those expected from the majority-spin subband.

SdH oscillations can be observed only if $\hbar\omega_c \gtrsim k_B T$ and $\omega_c\tau \gtrsim 1$, where ω_c is the cyclotron frequency, and τ is the relaxation time. In the present high-field experiments the first condition is well satisfied, but the second is probably met only barely. For a simple Drude model, and ignoring spin splitting, $\omega_c\tau=\mu H$, where μ is the Hall mobility. At 4.2 K and 100 kOe the Hall mobilities of the present metallic samples range between 3×10^2 and 6×10^2 cm^2/V s. These values lead to the estimates $\omega_c\tau=0.3$ to 0.6 at this temperature and field. Similar values are also obtained from the resistivity at $H=0$ and the carrier concentration (assumed to be equal to n_{RT} at room temperature). These rough estimates suggest that the requirement $\omega_c\tau \gtrsim 1$ was only marginally satisfied even in the high-field region where the oscillations were observed.

Model calculations were carried out using the following simplifying assumptions for the metallic samples. (1) The conduction band is parabolic, with an effective mass equal to that in the parent compound, $m^*=0.10m_0$. (2) The spin splitting δ in the field region where the oscillations are observed is approximated by a constant. This approximation is supported by the data of Isaacs *et al.*[22] For the present values of x we use $\delta=15$ meV. The small uncertainty in the value of δ, and the small uncertainty in m^*, have little effect on the results. (3) The carrier concentration n, which is the sum of the carrier concentrations n^+ and n^- in the two spin subbands, is constant and is equal to the room-temperature carrier concentration n_{RT}. This condition is used to calculate the Fermi level E_F. If E_F is measured from the bottom of the majority subband, then $E_F^+=E_F$ and $E_F^-=E_F-\delta$. These $E_F^\pm$ enter into the calculations of the periods ΔH^{-1} associated with the two subbands.

Two alternative approximate methods were used to calculate E_F. The first method assumes that E_F does not depend on H in the field range where δ is taken to be constant. An analogous assumption is often used in treating SdH oscillations.[32] The Fermi level is then calculated using the zero-field density of states $N(E)$ for each subband, except that the energy E is now measured from the bottom of the subband. In other words, the spin splitting of the CB is included but the structure in $N(E)$ due to the Landau quantization is ignored. The carrier concentrations n^+ and n^- are then independent of H (for a constant δ). The periods associated with the two subbands are (see Ref. 32, p. 171)

$$(\Delta H^{-1})_+=(e\hbar/m^*c)/E_F^+,\quad (\Delta H^{-1})_-=(e\hbar/m^*c)/E_F^-\ , \tag{10}$$

where standard notation is used.

This first method leads to the following results. For sample 4, with $n=2.9\times10^{17}$ cm^{-3}, the Fermi energy at $H=0$ is $E_F(0)=16.0$ meV. At high fields, $E_F^+=22.5$ meV, $E_F^-=7.5$ meV, $n^+=2.43\times10^{17}$ cm^{-3}, and $n^-=0.47\times10^{17}$ cm^{-3}. The period ΔH^{-1} from the majority subband is 5.1×10^{-6} Oe^{-1}, which is close to the observed value 4.8×10^{-6} Oe^{-1}. The minority subband gives rise to a period of 15.4×10^{-6} Oe^{-1}, which is much larger than observed. The Landau levels responsible for the observed oscillations are the $N=1$ and $N=2$ levels of the + subband (labeled hereafter as 1^+ and 2^+). These levels cross the Fermi level at $H_{1+}=130$ kOe and $H_{2+}=78$ kOe, which are roughly the fields of the observed resistivity maxima. For this particular sample the Landau level 0^-, in the minority subband, happens to cross the Fermi level at 130 kOe, which may enhance the effect of the 1^+ level.

Similar calculations for sample 5A give $\Delta H^{-1}=3.55\times10^{-6}$ Oe^{-1} for the majority subband, which agrees with the observed value 3.6×10^{-6} Oe^{-1}. The minority subband gives a period 6.6×10^{-6} Oe^{-1}. Again, the maxima of the oscillations in the MR are close to H_{1+} and H_{2+}. Landau level 1^- crosses the Fermi level at $H_{1-}=101$ kOe, which is not too far below $H_{2+}=113$ kOe. Thus, it is conceivable that the 1^- level enhances the effect of the 2^+ level. Landau level 0^- crosses at $H_{0-}=304$ kOe, which is far too high to affect the data. Similar results are also obtained for sample 5B. For this sample the calculated period for the majority subband is 3.3×10^{-6} Oe^{-1}, which is the same as the observed period.

The preceding results assumed that the Fermi level does not depend on H in the high-field region. This approximation is not fully justified when the SdH oscillations involve Landau levels with low quantum numbers. For this reason we also used a second approximate method. In this second method the effects of the Landau quantization on the density of states are included, but collision broadening of the Landau levels is neglected and T is set equal to zero. Numerical calculations using Eqs.

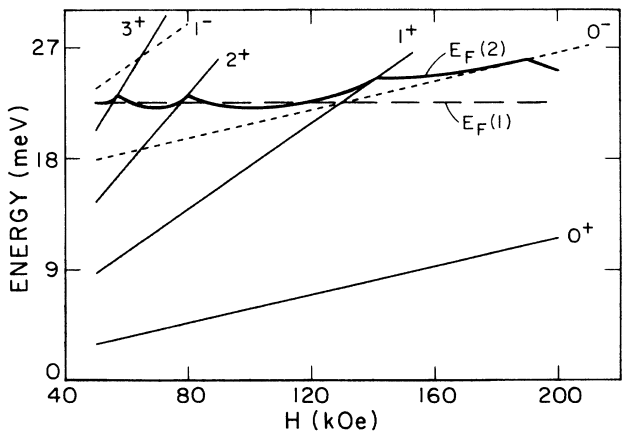

FIG. 12. Magnetic field dependence of the Fermi energy E_F, and energies of various Landau levels in the majority (+) and minority (−) spin subbands. The solid curve $E_F(2)$ is the Fermi energy calculated by the second method, while the horizontal dashed line $E_F(1)$ is the Fermi energy calculated by the first method (see text). All energies are relative to the bottom of the + subband. These results are for sample 4, with $n=2.9\times10^{17}$ cm^{-3}.

(5), (8a), and (23) of Ref. 32 then show that the Fermi level as well as the ratio n^-/n^+ oscillate with H. The oscillations of E_F change the fields at which the Landau levels cross the Fermi level. As a result, the periods from the majority and minority subbands are changed. In addition, the separation ΔH^{-1} between two successive crossings of the Fermi level by Landau levels of a given subband (i.e., the effective period in a particular field range) varies slightly with H at high fields.

Figure 12 shows results of numerical calculations for sample 4, using the second method. The variation of E_F with H shifts the fields H_{2+} and H_{1+} to 79.3 and 141.0 kOe, as compared to 77.9 and 129.8 kOe from the first method. The difference ΔH^{-1} is then 5.5×10^{-6} Oe^{-1}. This is still reasonably close to the observed period 4.8×10^{-6} Oe^{-1}. The crossing of the 0^- level is at $H_{0-}=189$ kOe, compared to 130 kOe from the first method. Since H_{0-} is now well above H_{1+}, the 0^- level will not enhance the MR oscillation caused by the 1^+ level.

Once the 0^- crosses the Fermi level, all the electrons are in the + subband. This is seen in Fig. 13 which shows n^-/n^+ as a function of H. The oscillations in n^-/n^+ for fields below 189 kOe correspond to a back-and-forth electron transfer between the two subbands. The peaks of n^-/n^+ in Fig. 13 correspond to H_{3+}, H_{2+}, and H_{1+}.

For sample 5A the second method gives $H_{1+}=197$ kOe and $H_{2+}=119$ kOe, compared to 188 and 113 kOe from the first method. The effective period from the majority subband is then $\Delta H^{-1}=3.3\times10^{-6}$ Oe^{-1}, which is only 8% below the observed period. The results for sample 5B are similar: the effective period is 3.1×10^{-6} Oe^{-1}, which is only 6% below the experimental value.

The two methods of calculating E_F represent two extremes. The first method neglects the change of E_F entirely. The second method, which neglects collision broadening and sets $T=0$, tends to exaggerate the oscillations of E_F with H. The actual situation is expected to be somewhere between these two extremes. Either method leads to a period from the majority subband which is close to that observed experimentally.

The temperature dependence of the amplitude of the SdH oscillations is governed by the factor $z/\sinh z$, where

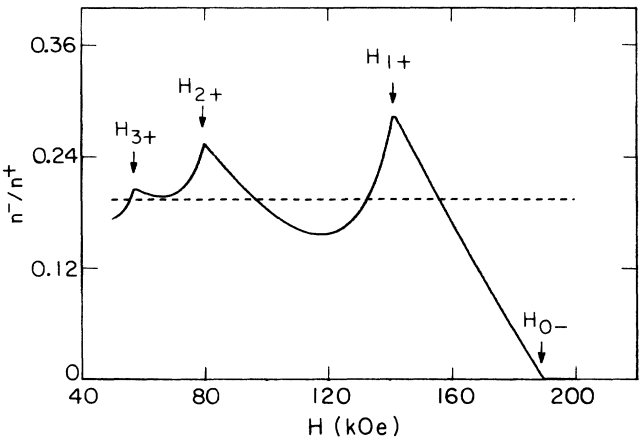

FIG. 13. Magnetic field dependence of the ratio n^-/n^+ between the electron concentrations in the minority and majority spin subbands. The solid curve is calculated using the second method, while the dashed line is from the first method (see text). The arrows mark the positions at which various Landau levels cross the Fermi level, as calculated by the second method. These results are for sample 4.

$z=2\pi^2k_BT/\hbar\omega_c$ (Ref. 32). Ordinarily, $z\gg1$ and the amplitude increases rapidly with decreasing T. In the present case, however, the ratio $\hbar\omega_c/k_BT$ is sufficiently large that $z<1$. As a result, the amplitude should increase only slightly with decreasing T. This agrees with the experimental observations.

ACKNOWLEDGMENTS

We are grateful to P. A. Lee and T. Dietl for useful discussions. The work at Tufts University was supported by the National Science Foundation (NSF) under Grant No. DMR-89-00419. The work at MIT was supported by NSF under Grant No. DMR-88-07419, and by the U.S. Defense Advanced Research Projects Agency (DARPA) under Grant No. N00014-86-0760. Travel funds for one of us (N.F.O.) were provided by Fundação de Amparo a Pesquisa do Estado de São Paulo (FAPESP), Brazil. The Francis Bitter National Magnet Laboratory is supported by NSF.

[1]S. Methfessel and D. C. Mattis, in *Handbuch der Physik*, edited by S. Flügge (Springer, Berlin, 1968), Vol. 18, Part 1.

[2]E. L. Nagaev, *Physics of Magnetic Semiconductors* (Mir, Moscow, 1983); Usp. Fiz. Nauk **117**, 437 (1975) [Sov. Phys.—Usp. **18**, 863 (1976)].

[3]J. K. Furdyna, J. Appl. Phys. **64**, R29 (1988).

[4]*Diluted Magnetic Semiconductors*, Vol. 25 of *Semiconductors and Semimetals*, edited by J. K. Furdyna and J. Kossut (Academic, New York, 1988).

[5]*Diluted Magnetic (Semimagnetic) Semiconductors*, edited by R. L. Aggarwal, J. K. Furdyna, and S. von Molnar (Materials Research Society, Pittsburgh, 1988).

[6]T. Dietl, J. Antoszewski, and L. Swierkowksi, Physica B+C **117B-118B**, 491 (1983).

[7]Y. Shapira, D. H. Ridgley, K. Dwight, A. Wold, K. P. Martin, J. S. Brooks, and P. A. Lee, Solid State Commun. **54**, 593 (1985); Y. Shapira, D. H. Ridgley, K. Dwight, A. Wold, K. P. Martin, and J. S. Brooks, J. Appl. Phys. **57**, 3210 (1985).

[8]M. Sawicki, T. Dietl, and J. Kossut, Acta Phys. Pol. A **67**, 399 (1985); M. Sawicki and T. Dietl, in *Proceedings of the 19th International Conference on the Physics of Semiconductors, Warsaw, 1988*, edited by W. Zawadzki (Polish Academy of Science, Warsaw, 1988), p. 1217.

[9]M. Sawicki, T. Dietl, J. Kossut, J. Igalson, T. Wojtowicz, and W. Plesiewicz, Phys. Rev. Lett. **56**, 508 (1986); T. Wojtowicz, T. Dietl, M. Sawicki, W. Plesiewicz, and J. Jaroszynski, *ibid.* **56**, 2419 (1986).

[10]J. Stankiewicz, S. von Molnar, and W. Giriat, Phys. Rev. B **33**, 3573 (1986).

[11]Y. Shapira, N. F. Oliveira, Jr., D. H. Ridgley, R. Kershaw, K. Dwight, and A. Wold, Phys. Rev. B **34**, 4187 (1986).

[12]Y. Shapira, in *Diluted Magnetic (Semimagnetic) Semiconduc-*

tors, edited by R. L. Aggarwal, J. K. Furdyna, and S. von Molnar (Materials Research Society, Pittsburgh, 1988), p. 209.

[13]T. Dietl, M. Sawicki, J. Jaroszynski, T. Wojtowicz, W. Plesiewicz, and A. Lenard, in *Proceedings of the 19th International Conference on the Physics of Semiconductors, Warsaw, 1988,* edited by W. Zawadzki (Polish Academy of Science, Warsaw, 1988), p. 1189.

[14]B. I. Shklovskii and A. L. Efros, *Electronic Properties of Doped Semiconductors* (Springer, Berlin, 1984).

[15]For a review, see J. Kossut, in *Diluted Magnetic Semiconductors,* Vol. 25 of *Semiconductors and Semimetals,* edited by J. K. Furdyna and J. Kossut (Academic, New York, 1988).

[16]Y. Shapira, S. Foner, D. H. Ridgley, K. Dwight, and A. Wold, Phys. Rev. B **30**, 4021 (1984); Y. Shapira and N. F. Oliveira, Jr., *ibid.* **35**, 6888 (1987); S. Foner, Y. Shapira, D. Heiman, P. Becla, R. Kershaw, K. Dwight, and A. Wold, *ibid.* **39**, 11 793 (1989).

[17]N. Yamada, S. Takeyama, T. Sakakibara, T. Goto, and N. Miura, Phys. Rev. B **34**, 4121 (1986).

[18]H. Fritzsche, in *The Metal Non-Metal Transition in Disordered Systems,* edited by L. R. Friedman and D. P. Tunstall (Scottish Universities Summer School in Physics, Edinburgh, 1978).

[19]B. Segall, in *Physics and Chemistry of II-VI Compounds,* edited by M. Aven and J. S. Prener (North-Holland, Amsterdam, 1967).

[20]B. Segall, M. R. Lorenz, and R. E. Halsted, Phys. Rev. **129**, 2471 (1963).

[21]J. A. Gaj, R. Planel, and G. Fishman, Solid State Commun. **29**, 435 (1979).

[22]D. L. Peterson, D. U. Bartholomew, U. Debska, A. K. Ramdas, and S. Rodriguez, Phys. Rev. B **32**, 323 (1985); E. D. Isaacs, D. Heiman, P. Becla, Y. Shapira, R. Kershaw, K. Dwight, and A. Wold, *ibid.* **38**, 8412 (1988).

[23]H. Fukuyama and K. Yosida, J. Phys. Soc. Jpn. **46**, 102 (1979).

[24]Y. Shapira and R. L. Kautz, Phys. Rev. B **10**, 4781 (1974); R. L. Kautz and Y. Shapira, in *Proceedings of the 20th Annual Conference on Magnetism and Magnetic Materials,* AIP Conf. Proc. No. 24, edited by C. D. Graham, G. H. Lander, and J. J. Rhyne (AIP, New York, 1975), p. 42.

[25]D. J. Kim and B. B. Schwartz, Phys. Rev. B **15**, 377 (1977).

[26]Z. Gan and P. A. Lee (unpublished).

[27]P. A. Lee and T. V. Ramakrishnan, Phys. Rev. B **26**, 4009 (1982).

[28]P. A. Lee and T. V. Ramakrishnan, Rev. Mod. Phys. **57**, 287 (1985).

[29]Y. Isawa, K. Hoshino, and H. Fukuyama, J. Phys. Soc. Jpn. **51**, 3262 (1982).

[30]T. F. Rosenbaum, R. F. Milligan, G. A. Thomas, P. A. Lee, T. V. Ramakrishnan, R. N. Bhatt, K. DeConde, H. Hess, and T. Perry, Phys. Rev. Lett. **47**, 1758 (1981).

[31]S. Morita, Y. Isawa, T. Fukase, S. Ishida, Y. Koike, Y. Takeuti, and N. Mikoshiba, Phys. Rev. B **25**, 5570 (1982).

[32]L. M. Roth and P. N. Argyres, in *Semiconductors and Semimetals,* edited by R. K. Willardson and A. C. Beer (Academic, New York, 1966), Vol. 1.